
Flag Aggregator: Scalable Distributed Training under Failures and Augmented Losses using Convex Optimization

Hamidreza Almasi Harsh Mishra Balajee Vamanan Sathya N. Ravi
 Department of Computer Science
 University of Illinois Chicago
 {halmas3, hmishr3, bvamanan, sathya}@uic.edu

Abstract

Modern ML applications increasingly rely on complex deep learning models and large datasets. There has been an exponential growth in the amount of computation needed to train the largest models. Therefore, to scale computation and data, these models are inevitably trained in a distributed manner in clusters of nodes, and their updates are aggregated before being applied to the model. However, a distributed setup is prone to Byzantine failures of individual nodes, components, and software. With data augmentation added to these settings, there is a critical need for robust and efficient aggregation systems. We define the quality of workers as reconstruction ratios $\in (0, 1]$, and formulate aggregation as a Maximum Likelihood Estimation procedure using Beta densities. We show that the Regularized form of log-likelihood wrt subspace can be approximately solved using iterative least squares solver, and provide convergence guarantees using recent Convex Optimization landscape results. Our empirical findings demonstrate that our approach significantly enhances the robustness of state-of-the-art Byzantine resilient aggregators. We evaluate our method in a distributed setup with a parameter server, and show simultaneous improvements in communication efficiency and accuracy across various tasks. The code is publicly available at <https://github.com/hamidralmasi/FlagAggregator>

1 Introduction

How to Design Aggregators? We consider the problem of designing aggregation functions that can be written as optimization problems of the form,

$$\mathcal{A}(g_1, \dots, g_p) \in \arg \min_{Y \in C} A_{g_1, \dots, g_p}(Y), \quad (1)$$

where $\{g_i\}_{i=1}^p \subseteq \mathbb{R}^n$ are given estimates of an unknown summary statistic used to compute the Aggregator Y^* . If we choose A to be a quadratic function that decomposes over g_i 's, and $C = \mathbb{R}^n$, then we can see \mathcal{A} is simply the standard mean operator. There is a mature literature of studying such functions for various scientific computing applications [1]. More recently, from the machine learning standpoint there has been a plethora of work [2, 3, 4, 5] on designing provably robust aggregators \mathcal{A} for mean estimation tasks under various technical assumptions on the distribution or moments of g_i .

Distributed ML Use Cases. Consider training a model with a large dataset such as ImageNet-1K [6] or its augmented version which would require data to be distributed over p workers and uses back propagation. Indeed, in this case, g_i 's are typically the gradients computed by individual workers at each iteration. In settings where the training objective is convex, the convergence and generalization properties of distributed optimization can be achieved by defining \mathcal{A} as a weighted

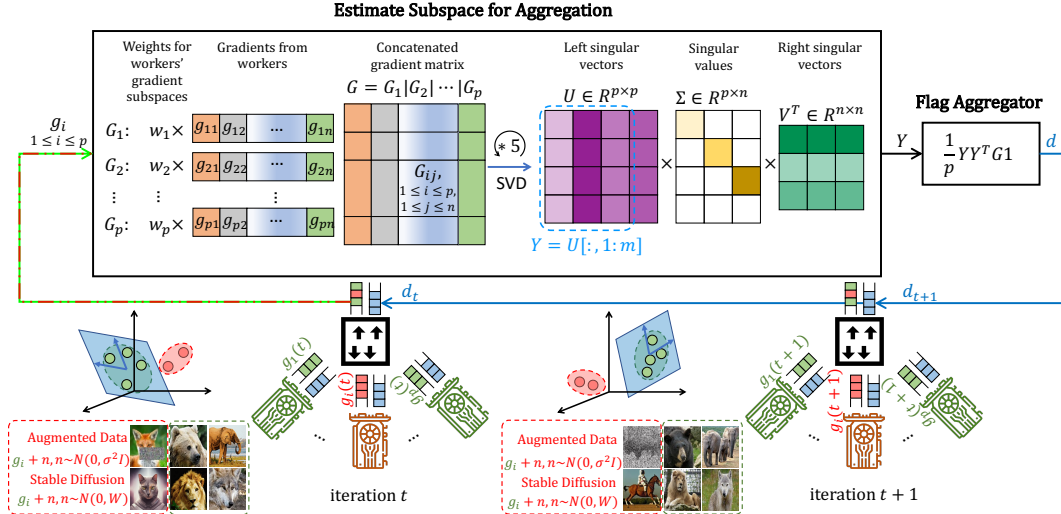


Figure 1: Robust gradient aggregation in our distributed training framework. In our applications, each of the p workers provides gradients computed using a random sample obtained from given training data, derived synthetic data from off-the-shelf Diffusion models, and random noise in each iteration. Our Flag Aggregator (FA) removes high frequency noise components by using few rounds of Singular Value Decomposition of the concatenated Gradient Matrix G , and provides new update Y^* .

combination of gradients facilitated by a simple consensus matrix, even if some g_i 's are noisy [7, 8]. In a distributed setup, as long as the model is convex we can simultaneously minimize the total iteration or communication complexity to a significant extent i.e., it is possible to achieve convergence *and* robustness under technical assumptions on the moments of (unknown) distribution from which g_i 's are drawn. However, it is still an open problem to determine the optimality of these procedures in terms of either convergence or robustness [9, 10].

Potential Causes of Noise. When data is distributed among workers, hardware and software failures in workers [11, 12, 13] can cause them to send incorrect gradients, which can significantly mislead the model [14]. To see this, let's consider a simple experiment with 15 workers, that f of them produce uniformly random gradients. Figure 2 shows that the model accuracy is heavily impacted when $f > 0$ when mean is used to aggregate the gradients.

The failures can occur due to component or software failures and their probability increases with the scale of the system [15, 16, 17]. Reliability theory is used to analyze such failures, see Chapter 9 in [18], but for large-scale training, the distribution of total system failures is not independent over workers, making the total noise in gradients dependent and a key challenge for large-scale training. Moreover, even if there are no issues with the infrastructure, our work is motivated by the prevalence of data augmentation, including hand-chosen augmentations. Since number of parameters n is often greater than number of samples, data augmentation improves the generalization capabilities of large-scale models under technical conditions [19, 20, 21]. In particular, Adversarial training is a common technique that finds samples that are close to training samples but classified as a different class at the current set of parameters, and then use such samples for parameter update purposes [22]. Unfortunately, computing adversarial samples is often difficult [23], done using randomized algorithms [24] and so may introduce dependent (across samples) noise themselves. In other words, using adversarial training paradigm, or the so-called inner optimization can lead to noise in gradients, which can cause or simulate dependent "Byzantine" failures in the distributed context.

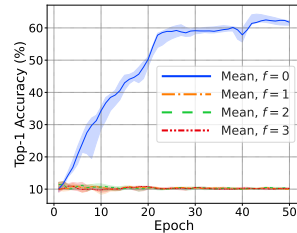


Figure 2: Tolerance to f Byzantine workers for a non-robust aggregator (mean).

Available Computational Solutions. Most existing open source implementations of \mathcal{A} rely just on (functions of) pairwise distances to filter gradients from workers using suitable neighborhood

based thresholding schemes, based on moment conditions [25, 26, 27]. While these may be a good strategy when the noise in samples/gradients is somewhat independent, these methods are suboptimal when the noise is dependent or nonlinear, especially when n is large. Moreover, choosing discrete hyperparameters such as number of neighbors is impractical in our use cases since they hamper convergence of the overall training procedure. To mitigate the suboptimality of existing aggregation schemes, we explicitly estimate a subspace Y spanned by “most” of the gradient workers, and then use this subspace to estimate that a **sparse** linear combination of g_i gradients, achieving robustness.

We present a new optimization based formulation for generalized gradient aggregation purposes in the context of distributed training of deep learning architectures, as shown in Figure 1.

Summary of our Contributions. From the theoretical perspective, we present a simple Maximum Likelihood Based estimation procedure for aggregation purposes, with novel regularization functions. Algorithmically, we argue that any procedure used to solve Flag Optimization can be directly used to obtain the optimal summary statistic Y^* for our aggregation purposes. **Experimentally**, our results show resilience against Byzantine attacks, encompassing physical failures, while effectively managing the stochasticity arising from data augmentation schemes. In practice, we achieve a *significantly* ($\approx 20\%$) better accuracy on standard datasets. Our **implementation** offers substantial advantages in reducing communication complexity across diverse noise settings through the utilization of our novel aggregation function, making it applicable in numerous scenarios.

2 Robust Aggregators as Orthogonality Constrained Optimization

In this section, we first provide the basic intuition of our proposed approach to using subspaces for aggregation purposes using linear algebra, along with connections of our approach standard eigendecomposition based denoising approaches. We then present our overall optimization formulation in two steps, and argue that it can be optimized using existing methods.

2.1 Optimal Subspace Hypothesis for Distributed Descent

We will use lowercase letters y, g to denote vectors, and uppercase letters Y, G to denote matrices. We will use **boldfont 1** to denote the vector of all ones in appropriate dimensions. Let $g_i \in \mathbb{R}^n$ be the gradient vector from worker i , and $Y \in \mathbb{R}^{n \times m}$ is an orthogonal matrix representation of a subspace that gradients could live in such that $m \leq p$. Now, we may interpret each column of Y as a basis function that act on $g_i \in \mathbb{R}^n$, i.e., j -th coordinate of $(Y^T g)_j$ for $1 \leq j \leq m$ is the application of j -th basis or column of Y on g . Recall that by definition of dot product, we have that if $Y_{:,j} \perp g$, then $(Y^T g)_j$ will be close to zero. Equivalently, if $g \in \text{span}(Y)$, then $(Y^T g)^T Y^T g$ will be bounded away from zero, see Chapter 2 in [28]. Assuming that $G \in \mathbb{R}^{n \times p}$ is the gradient matrix of p workers, $Y Y^T G \in \mathbb{R}^{n \times p}$ is the reconstruction of G using Y as basis. That is, i^{th} column of $Y^T G$ specifies the amount of gradient from worker i as a function of Y , and high l_2 norm of $Y^T g_i$ implies that there is a basis in Y such that $Y \not\perp g_i$. So it is easy to see that the average over columns of $Y Y^T G$ would give the final gradient for update.

Explained Variance of worker i . If we denote $z_i = Y^T g_i \in \mathbb{R}^m$ representing the transformation of gradient g_i to z_i using Y , then, $0 \leq \|z_i\|_2^2 = z_i^T z_i = (Y^T g)^T Y^T g = g_i^T Y Y^T g_i$ is a scalar, and so is equal to its trace $\text{tr}(g_i^T Y Y^T g_i)$. Moreover, when Y is orthogonal, we have $0 \leq \|z_i\|_2 = \|Y^T g_i\|_2 \leq \|Y\|_2 \|g_i\|_2 \leq \|g_i\|_2$ since the operator norm (or largest singular value) $\|Y\|_2$ of Y is at most 1. Our main idea is to use $\|z_i\|_2^2, \|g_i\|_2^2$ to define the quality of the subspace Y for aggregation, as is done in some previous works for Robust Principal Component Estimation [29] – the quantity $\|z_i\|_2^2 / \|g_i\|_2^2$ is called as *Explained/Expressed* variance of subspace Y wrt i -th worker [30, 31] – we refer to $\|z_i\|_2^2 / \|g_i\|_2^2$ as the “value” of i -th worker. In Figure 3, we can see from the spike near 1.0 that if we choose the subspace carefully (blue) as opposed to merely choosing the mean gradient (with unit norm) of all workers, then we can increase the value of workers.

Advantages of Subspace based Aggregation. We can see that using subspace Y , we can easily: 1. handle different number of gradients from each worker, 2. compute gradient reconstruction $Y Y^T G$

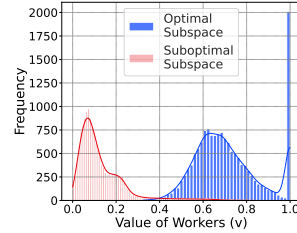


Figure 3: Distributions of Explained Variances on Minibatches

efficiently whenever Y is constrained to be orthogonal $Y = \sum_i y_i y_i^T$ where y_i is the i -th column of Y , otherwise have to use eigendecomposition of Y to measure explained variance which can be time consuming. In (practical) distributed settings, the quality (or noise level) of gradients in each worker may be different, **and/or** each worker may use a different batch size. In such cases, handcrafted aggregation schemes may be difficult to maintain, and fine-tune. For these purposes with an Orthogonal Subspace Y , we can simply reweigh gradients of worker i according to its noise level, **and/or** use $g_i \in \mathbb{R}^{n \times b_i}$ where b_i is the batch size of i -th worker with $\text{tr}(z_i^T z_i)$ instead.

Why is optimizing over subspaces called “Flag” Optimization? Recent optimization results suggest that we can exploit the finer structure available in Flag Manifold to specify Y more precisely [32]. For example, $Y \in \mathbb{R}^{n \times m}$ can be parametrized directly as a subspace of dimension m or as a nested sequence of $Y_k \in \mathbb{R}^{n \times m_k}$, $k = 1, \dots, K$ where $m_k < m_{k+1} \leq p \leq n$ such that $\text{span}(Y_k) \subseteq \text{span}(Y_{k+1})$ with $Y_K \in \mathbb{R}^{n \times m}$. When $m_{k+1} = m_k = 1$, we have the usual (real) Grassmanian Manifold (quotient of orthogonal group) whose coordinates can be used for optimization, please see Section 5 in [33] for details. In fact, [34] used this idea to extend median in one-dimensional vector spaces to different finite dimensional *subspaces* using the so-called chordal distance between them. In our distributed training context, we use the explained variance of each worker instead. Here, workers may specify dimensions along which gradient information is relevant for faster convergence – an advantage currently not available in existing aggregation implementations – which may be used for smart initialization also. We use “Flag” to emphasize this additional nested structure available in our formulation for distributed training purposes.

2.2 Approximate Maximum Likelihood Estimation of Optimal Subspace

Now that we can evaluate a subspace Y on individual gradients g_i , we now show that finding subspace Y can be formulated using standard maximum likelihood estimation principles [35]. Our formulation reveals that regularization is critical for aggregation especially in distributed training. In order to write down the objective function for finding optimal Y , we proceed in the following two steps:

Step 1. Assume that each worker provides a single gradient for simplicity. Now, denoting the value of information v of worker i by $v_i = \frac{z_i^T z_i}{g_i^T g_i}$, we have $v_i \in [0, 1]$. Now by assuming that v_i 's are observed from Beta distribution with $\alpha = 1$ and $\beta = \frac{1}{2}$ (for simplicity), we can see that the likelihood $\mathbb{P}(v_i)$ is,

$$\mathbb{P}(v_i) := \frac{(1 - v_i)^{-\frac{1}{2}}}{B(1, \frac{1}{2})} = \frac{\left(1 - \frac{z_i^T z_i}{g_i^T g_i}\right)^{-\frac{1}{2}}}{B(1, \frac{1}{2})}, \quad (2)$$

where $B(a, b)$ is the normalization constant. Then, the total log-likelihood of observing gradients g_i as a function of Y (or v_i 's) is given by taking the log of product of $\mathbb{P}(v_i)$'s as (ignoring constants),

$$\log \left(\prod_{i=1}^p \mathbb{P}(v_i) \right) = \sum_{i=1}^p \log(\mathbb{P}(v_i)) = -\frac{1}{2} \sum_{i=1}^p \log(1 - v_i). \quad (3)$$

Step 2. Now we use Taylor's series with constant $a > 0$ to approximate individual worker log-likelihoods $\log(1 - v_i) \approx a(1 - v_i)^{\frac{1}{a}} - a$ as follows: first, we know that $\exp\left(\frac{\log(v_i)}{a}\right) = v_i^{\frac{1}{a}}$. On the other hand, using Taylor expansion of \exp about the origin (so large $a > 1$ is better), we have that $\exp\left(\frac{\log(v_i)}{a}\right) \approx 1 + \frac{\log(v_i)}{a}$. Whence, we have that $1 + \frac{\log(v_i)}{a} \approx v_i^{\frac{1}{a}}$ which immediately implies that $\log(v_i) \approx a v_i^{\frac{1}{a}} - a$. So, by substituting the Taylor series approximation of \log in Equation 3, we obtain the *negative* log-likelihood approximation to be *minimized* for robust aggregation purposes as,

$$-\log \left(\prod_{i=1}^p \mathbb{P}(v_i) \right) \approx \frac{1}{2} \sum_{i=1}^p \left(a(1 - v_i)^{\frac{1}{a}} - a \right), \quad (4)$$

where $a > 1$ is a sufficiently large constant. In the above mentioned steps, the first step is standard. Our key insight is using Taylor expansion in (4) with a sufficiently large a to eliminate log optimization which are known to be computationally expensive to solve, and instead solve *smooth* $\ell_{a, a > 1}$ norm based optimization problems which can be done efficiently by modifying existing procedures [36].

Extension to general beta distributions, and gradients $\alpha > 0, \beta > 0, g_i \in \mathbb{R}^{n \times k}$. Note that our derivation in the above two steps can be extended to any beta shape parameters $\alpha > 0, \beta > 0$ – there

will be two terms in the final negative log-likelihood expression in our formulation (4), one for each α, β . Similarly, by simply using $v_i = \text{tr}(g_i^T Y Y^T g_i)$ to define value of worker i in equation (2), and then in our estimator in (4), we can easily handle multiple k gradients from a single worker i for Y .

2.3 Flag Aggregator for Distributed Optimization

It is now easy to see that by choosing $a = 2$, in equation (4), we obtain the negative loglikelihood (ignoring constants) as $(\sum_{i=1}^p \sqrt{1 - g_i^T Y Y^T g_i})$ showing that Flag Median can indeed be seen as an Maximum Likelihood Estimator (MLE). In particular, Flag Median can be seen as an MLE of Beta Distribution with parameters $\alpha = 1$ and $\beta = \frac{1}{2}$. Recent results suggest that in many cases, MLE is ill-posed, and regularization is necessary, even when the likelihood distribution is Gaussian [37]. So, based on the Flag Median estimator for subspaces, we propose an optimization based subspace estimator Y^* for aggregation purposes. We formulate our Flag Aggregator (FA) objective function with respect to Y as a *regularized* sum of likelihood based (or data) terms in (4) using trace operators $\text{tr}(\cdot)$ as the solution to the following constrained optimization problem:

$$\min_{Y: Y^T Y = I} A(Y) := \sum_{i=1}^p \sqrt{\left(1 - \frac{\text{tr}(Y^T g_i g_i^T Y)}{\|g_i\|_2^2}\right)} + \lambda \mathcal{R}(Y) \quad (5)$$

where $\lambda > 0$ is a regularization hyperparameter. In our analysis, and implementation, we provide support for two possible choices for $\mathcal{R}(Y)$:

- (1) **Mathematical norms:** $\mathcal{R}(Y)$ can be a form of norm-based regularization other than $\|Y\|_{\text{Fro}}^2$ since it is constant over the feasible set in (5). For example, it could be convex norm with efficient subgradient oracle such as, i.e. element-wise: $\sum_{i=1}^n \sum_{j=1}^m \|Y_{ij}\|_1$ or $\sum_{i=1}^m \|Y_{:,i}\|_1$.
- (2) **Data-dependent norms:** Following our subspace construction in Section 2.1, we may choose $\mathcal{R}(Y) = \frac{1}{p-1} \sum_{i,j=1, i \neq j}^p \sqrt{\left(1 - \frac{\text{tr}(Y^T (g_i - g_j)(g_i - g_j)^T Y)}{D_{ij}^2}\right)}$ where $D_{ij}^2 = \|g_i - g_j\|_2^2$ denotes the distance between gradient vectors g_i, g_j from workers i, j . Intuitively, the pairwise terms in our loss function (5) favors subspace Y that also reconstructs the pairwise vectors $g_i - g_j$ that are close to each other. So, by setting $\lambda = \Theta(p)$, that is, the pairwise terms dominate the objective function in (5). Hence, λ regularizes optimal solutions Y^* of (5) to contain g_i 's with low pairwise distance in its span – similar in spirit to AggregaThor in [38].

Convergence of Flag Aggregator (FA) Algorithm 1. With these, we can state our main algorithmic result showing that our FA (5) can be solved efficiently using standard convex optimization proof techniques. In particular, in supplement, we present a smooth Semi-Definite Programming (SDP) relaxation of FA in equation (5) using the Flag structure. This allows us to view the IRLS procedure in 1 as solving the low rank parametrization of the smooth SDP relaxation, thus guaranteeing fast convergence to second order optimal (local) solutions. Importantly, our SDP based proof works for any degree of approximation of the constant a in equation (4) and only relies on smoothness of the loss function wrt Y , although speed of convergence is reduced for higher values of $a \neq 2$, see [39]. We leave determining the exact dependence of a on rate of convergence for future work.

How is FA aggregator different from (Bulyan and Multi-Krum)? Bulyan is a strong Byzantine resilient gradient aggregation rule for $p \geq 4f + 3$ where p is the total number of workers and f is the number of Byzantine workers. Bulyan is a two-stage algorithm. In the first stage, a gradient aggregation rule R like coordinate-wise median [40] or Krum [9] is recursively used to select $\theta = p - 2f$ gradients. The process uses R to select gradient vector g_i which is closest to R 's output (e.g. for Krum, this would be the gradient with the top score, and hence the exact output of R). The chosen gradient is removed from the received set and added to the selection set S repeatedly until $|S| = \theta$. The second stage produces the resulting gradient. If $\beta = \theta - 2f$, each coordinate would be the average of β -nearest to the median coordinate of the θ gradients in S . In matrix terms, if we consider $S \in \mathbb{R}^{p \times m}$ as a matrix with each column having one non-zero entry summing to 1, Bulyan would return $\frac{1}{m} \text{ReLU}(GS)\mathbf{1}_m$, where $\mathbf{1}_m \in \mathbb{R}^m$ is the vector of all ones, while FA would return $\frac{1}{p} Y Y^T G \mathbf{1}_p$. Importantly, the gradient matrix is being right-multiplied in Bulyan, but left-multiplied in FA, before getting averaged. While this may seem like a discrepancy, in supplement we show that by observing the optimality conditions of (5) wrt Y , we show that $\frac{1}{m} Y Y^T G$ can be seen as a right

Algorithm 1 Distributed SGD with proposed Flag Aggregator (FA) at the Parameter Server

Input: Number of workers p , loss functions l_1, l_2, \dots, l_p , per-worker minibatch size B , learning rate schedule α_t , initial parameters w_0 , number of iterations T

Output: Updated parameters w_T from any worker

```
1 for  $t = 1$  to  $T$  do
2   for  $p = 1$  to  $p$  in parallel on machine  $p$  do
3     Select a minibatch:  $i_{p,1,t}, i_{p,2,t}, \dots, i_{p,B,t}$   $g_{p,t} \leftarrow \frac{1}{B} \sum_{b=1}^B \nabla l_{i_{p,b,t}}(w_{t-1})$ 
4      $G_t \leftarrow \{g_{1,t}, \dots, g_{p,t}\}$  // Parameter Server receives gradients from  $p$  workers
5      $\hat{Y}_t \leftarrow$  IRLS( $\hat{G}_t$ ) with  $\hat{G}_t = G_t + \lambda \nabla \mathcal{R}(Y) \mathbf{1}^T$  // Do IRLS at the Parameter Server for  $\hat{Y}$ 
6     Obtain gradient direction  $d_t$ :  $d_t = \frac{1}{p} \hat{Y}_t \hat{Y}_t^T G_t \mathbf{1}$  // Compute, Send  $d_t$  to all  $p$  machines
7     for  $p = 1$  to  $p$  in parallel on machine  $p$  do
8       update model:  $w_t \leftarrow w_{t-1} - \alpha_t \cdot d_t$ 
9 Return  $w_T$ 
```

multiplication by a matrix parametrized by lagrangian multipliers associated with the orthogonality constraints in (5). This means it should be possible to combine both approaches for faster aggregation.

3 Experiments

In this section, we conduct experiments to test our proposed FA in the context of distributed training in two testbeds. First, to test the performance of our FA scheme solved using IRLS (Flag Mean) on standard Byzantine benchmarks. Then, to evaluate the ability of existing state-of-the-art gradient aggregators we augment data via two techniques that can be implemented with Sci-kit package.

Implementation Details. We implement FA in Pytorch [41], which is popular but does not support Byzantine resilience natively. We adopt the parameter server architecture and employ Pytorch’s distributed RPC framework with TensorPipe backend for machine-to-machine communication. We extend Garfield’s Pytorch library [42] with FA and limit our IRLS convergence criteria to a small error, 10^{-10} , or 5 iterations of flag mean for SVD calculation. We set $m = \lceil \frac{p+1}{2} \rceil$.

3.1 Setup

Baselines: We compare FA to several existing aggregation rules: (1) coordinate-wise **Trimmed Mean** [40] (2) coordinate-wise **Median** [40] (3) mean-around-median (**MeaMed**) [43] (4) **Phocas** [44] (5) **Multi-Krum** [9] (6) **Bulyan** [45].

Accuracy: The fraction of correct predictions among all predictions, using the test dataset (top-1 cross-accuracy).

Testbed: We used 4 servers as our experimental platform. Each server has 2 Intel(R) Xeon(R) Gold 6240 18-core CPU @ 2.60GHz with Hyper-Threading and 384GB of RAM. Servers have a Tesla V100 PCIe 32GB GPU and employ a Mellanox ConnectX-5 100Gbps NIC to connect to a switch. We use one of the servers as the parameter server and instantiate 15 workers on other servers, each hosting 5 worker nodes, unless specified differently in specific experiments. For the experiments designed to show scalability, we instantiate 60 workers.

Dataset and model: We focus on the image classification task since it is a widely used task for benchmarking in distributed training [46]. We train ResNet-18 [47] on CIFAR-10 [48] which has 60,000 32×32 color images in 10 classes. For the scalability experiment, we train a CNN with two convolutional layers followed by two fully connected layers on MNIST [49] which has 70,000 28×28 grayscale images in 10 classes. We also run another set of experiments on Tiny ImageNet [50] in the supplement. We use SGD as the optimizer, and cross-entropy to measure loss. The batch size for each worker is 128 unless otherwise stated. Also, we use a learning decay strategy where we decrease the learning rate by a factor of 0.2 every 10 epochs.

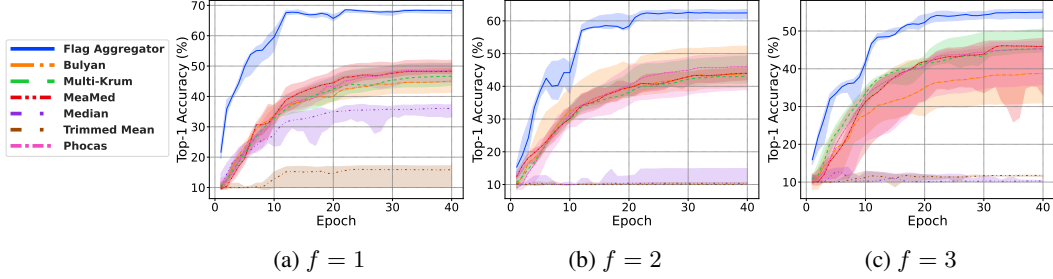


Figure 4: Tolerance to the number of Byzantine workers for robust aggregators for batch size 128.

Threat models: We evaluate FA under two classes of Byzantine workers. They can send uniformly random gradients that are representative of errors in the physical setting, or use non-linear augmented data described as below.

Evaluating resilience against nonlinear data augmentation: In order to induce Byzantine behavior in our workers we utilize ODE solvers to approximately solve 2 non-linear processes, Lotka Volterra [51] and Arnold’s Cat Map [52], as augmentation methods. Since the augmented samples are deterministic, albeit nonlinear functions of training samples, the “noise” is dependent across samples.

In **Lotka Volterra**, we use the following linear gradient transformation of 2D pixels:

$$(x, y) \rightarrow (\alpha x - \beta xy, \delta xy - \gamma y),$$

where α, β, γ and δ are hyperparameters. We choose them to be $\frac{2}{3}, \frac{4}{3}, -1$ and -1 respectively.

Second, we use a *nonsmooth* transformation called **Arnold’s Cat Map** as a data augmentation scheme. Once again, the map can be specified using a two-dimensional matrix as,

$$(x, y) \rightarrow \left(\frac{2x + y}{N}, \frac{x + y}{N} \right) \bmod 1,$$

where \bmod represents the modulus operation, x and y are the coordinates or pixels of images and N is the height/width of images (assumed to be square). We also used a smooth approximation of the Cat Map obtained by approximating the \bmod function as,

$$(x, y) \rightarrow \frac{1}{n} \left(\frac{2x + y}{(1 + \exp(-m \log(\alpha_1)))}, \frac{x + y}{(1 + \exp(-m \log(\alpha_2)))} \right),$$

where $\alpha_1 = \frac{2x+y}{n}, \alpha_2 = \frac{x+y}{n}$, and m is the degree of approximation, which we choose to be 0.95 in our data augmentation experiments.

How to perform nonlinear data augmentation? In all three cases, we used SciPy’s [53] `solve_ivp` method to solve the differential equations, by using the LSODA solver. In addition to the setup described above, we also added a varying level of Gaussian noise to each of the training images. All the images in the training set are randomly chosen to be augmented with varying noise levels of the above mentioned augmentation schemes. We have provided the code that implements all our data augmentation schemes in the supplement zipped folder.

3.2 Results

Tolerance to the number of Byzantine workers: In this experiment, we show the effect of Byzantine behavior on the convergence of different gradient aggregation rules in comparison to FA. Byzantine workers send random gradients and we vary the number of them from 1 to 3. Figure 4 shows that for some rules, i.e. Trimmed Mean, the presence of even a single Byzantine worker has a catastrophic impact. For other rules, as the number of Byzantine workers increases, filtering out the outliers becomes more challenging because the amount of noise increases. Regardless, FA remains more robust compared to other approaches.

Marginal utility of larger batch sizes under a fixed noise level:

We empirically verified the batch size required to identify our optimal Y^* - the FA matrix at each iteration. In particular, we fixed the noise level to $f = 3$ Byzantine workers and varied batch sizes.

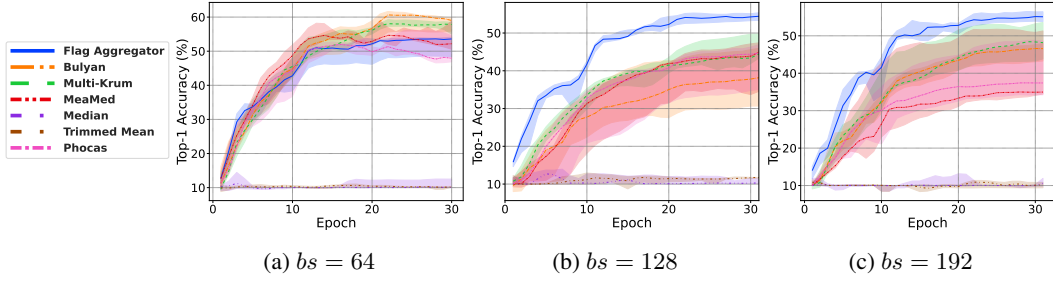


Figure 5: Marginal utility of larger batch sizes under a fixed noise level $f = 3$.

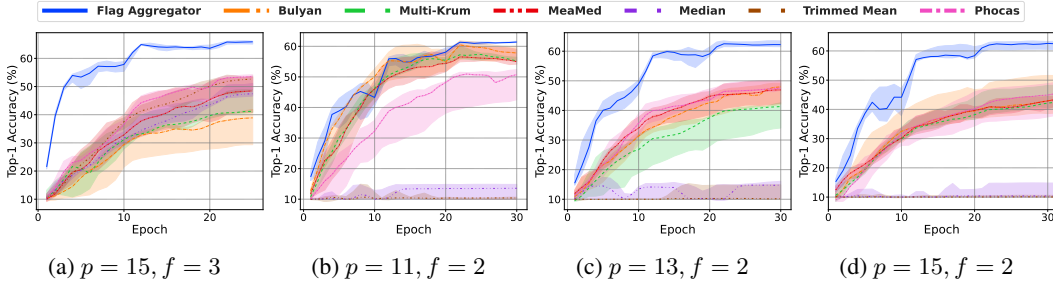


Figure 6: We present results under two different gradient attacks. The attack in (a) corresponds to simply dropping 10% of gradients from f workers. The attacks in (b)-(d) correspond to generic f workers sending random gradient vectors, i.e. we simply fix noise level while adding more workers.

We show the results in Figure 5. **Our results indicate that, in cases where a larger batch size is a training requirement, FA achieves a significantly better accuracy compared to the existing state of the art aggregators.** This may be useful in some large scale vision applications, see [54, 55] for more details. Empirically, we can already see that our spectral relaxation to identify gradient subspace is effective in practice in all our experiments.

Tolerance to communication loss: To analyze the effect of unreliable communication channels between the workers and the parameter server on convergence, we design an experiment where the physical link between some of the workers and the parameter server randomly drops a percentage of packets. Here, we set the loss rate of three links to 10% i.e., there are 3 Byzantine workers in our setting. The loss is introduced using the *netem* queuing discipline in Linux designed to emulate the properties of wide area networks [56]. The two main takeaways in Figure 6a are:

1. FA converges to a significantly higher accuracy than other aggregators, and thus is more robust to unreliable underlying network transports.
2. Considering time-to-accuracy for comparison, FA reaches a similar accuracy in less total number of training iterations, and thus is more robust to slow underlying network transports.

Analyzing the marginal utility of additional workers. To see the effect of adding more workers to a fixed number of Byzantine workers, we ran experiments where we fixed f , and increased p . Our experimental results shown in Figures 6b-6d indicate that our FA algorithm possesses strong resilience property for reasonable choices of p .

The effect of having augmented data during training in Byzantine workers: Figure 7 shows FA can handle nonlinear data augmentation in a much more stable fashion. Please see supplement for details on the level of noise, and exact solver settings that were used to obtain augmented images.

The effect of the regularization parameter in FA: The data-dependent regularization parameter λ in FA provides flexibility in the loss function to cover aggregators that benefit from pairwise distances such as Bulyan and Multi-Krum. To verify whether varying λ can interpolate Bulyan and Multi-Krum, we change λ in Figure 8. We can see when FA improves or performs similarly for a range of λ . Here, we set p and f to satisfy the strong Byzantine resilience condition of Bulyan, i.e. $p \geq 4f + 3$.

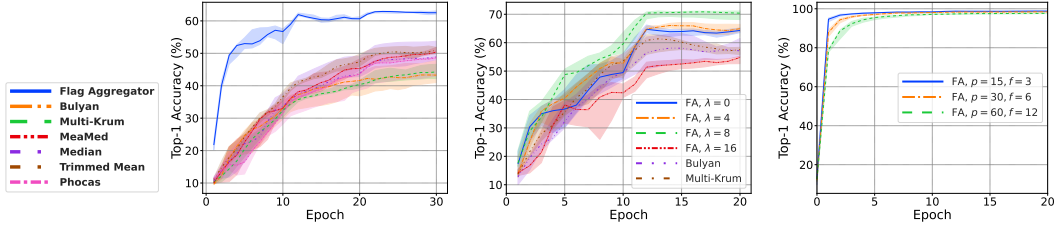


Figure 7: Accuracy of using augmented data in $f = 3$ workers
 Figure 8: CIFAR-10 with ResNet-18, $p = 7$, and $f = 1$
 Figure 9: Scaling FA to larger setups

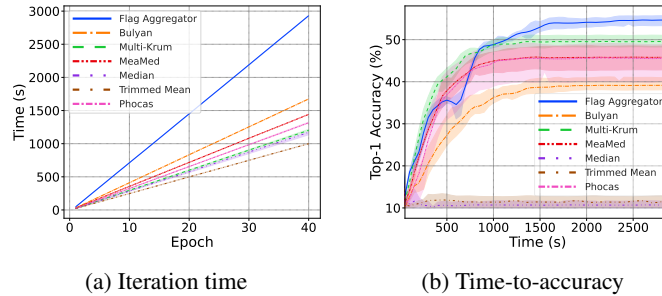


Figure 10: Wall clock time comparison

Scaling out to real-world situations with more workers: In distributed ML, p and f are usually large. To test high-dimensional settings commonly dealt in Semantic Vision with our FA, we used ResNet-18. Now, to specifically test the scalability of FA, we fully utilized our available GPU servers and set up to $p = 60$ workers (up to $f = 14$ Byzantine) with the MNIST dataset and a simple CNN with two convolutional layers followed by two fully connected layers (useful for simple detection). Figure 9 shows evidence that FA is feasible for larger setups.

4 Discussion and Limitation

Is it possible to fully “offload” FA computation to switches? Recent work propose that aggregation be performed entirely on network infrastructure to alleviate any communication bottleneck that may arise [57, 58]. However, to the best of our knowledge, switches that are in use today only allow limited computation to be performed on gradient g_i as packets whenever they are transmitted [59, 60]. That is, *programmability* is restrictive at the moment— switches used in practice have no floating point, or loop support, and are severely memory/state constrained. Fortunately, solutions seem near. For instance, [61] have already introduced support for floating point arithmetic in programmable switches. We may use quantization approaches for SVD calculation with some accuracy loss [62] to approximate floating point arithmetic. Offloading FA to switches has great potential in improving its computational complexity because the switch would perform as a high-throughput streaming parameter server to synchronize gradients over the network. Considering that FA’s accuracy currently outperforms its competition in several experiments, an offloaded FA can reach their accuracy even faster or it could reach a higher accuracy in the same amount of time.

Potential Limitation. Because in every iteration of FA, we perform SVD, the complexity of the algorithm would be $O(nN_\delta(\sum_{i=1}^p k_i)^2)$ with N_δ being the number of iterations for the algorithm. Figure 10 shows the wall clock time it takes for FA to reach a certain epoch (10a) or accuracy (10b) compared to other methods under a fixed amount of random noise $f = 3$ with $p = 15$ workers. Although the iteration complexity of FA is higher, here each iteration has a higher utility as reflected in the time-to-accuracy measures. This makes FA comparable to others in a shorter time span, however, if there is more wall clock time to spare, FA converges to a better state as shown in Figure 10b.

5 Conclusion

In this paper we proposed Flag Aggregator (FA) that can be used for robust aggregation of gradients in distributed training. FA is an optimization-based subspace estimator that formulates aggregation as a Maximum Likelihood Estimation procedure using Beta densities. We perform extensive evaluations of FA and show it can be effectively used in providing Byzantine resilience for gradient aggregation. Using techniques from convex optimization, we theoretically analyze FA and with tractable relaxations show its amenability to be solved by off-the-shelf solvers or first-order reweighing methods.

References

- [1] Michel Grabisch, Jean-Luc Marichal, Radko Mesiar, and Endre Pap. *Aggregation functions*, volume 127. Cambridge University Press, 2009.
- [2] Sivaraman Balakrishnan, Simon S. Du, Jerry Li, and Aarti Singh. Computationally efficient robust sparse estimation in high dimensions. In Satyen Kale and Ohad Shamir, editors, *Proceedings of the 2017 Conference on Learning Theory*, volume 65 of *Proceedings of Machine Learning Research*, pages 169–212. PMLR, 07–10 Jul 2017. URL <https://proceedings.mlr.press/v65/balakrishnan17a.html>.
- [3] Ilias Diakonikolas, Daniel Kane, Sushrut Karmalkar, Eric Price, and Alistair Stewart. Outlier-robust high-dimensional sparse estimation via iterative filtering. *Advances in Neural Information Processing Systems*, 32, 2019.
- [4] Yu Cheng, Ilias Diakonikolas, Rong Ge, Shivam Gupta, Daniel M. Kane, and Mahdi Soltanolkotabi. Outlier-robust sparse estimation via non-convex optimization. *Advances in Neural Information Processing Systems*, 2022.
- [5] Ilias Diakonikolas, Daniel M. Kane, Sushrut Karmalkar, Ankit Pensia, and Thanasis Pappas. Robust sparse mean estimation via sum of squares. In Po-Ling Loh and Maxim Raginsky, editors, *Proceedings of Thirty Fifth Conference on Learning Theory*, volume 178 of *Proceedings of Machine Learning Research*, pages 4703–4763. PMLR, 02–05 Jul 2022. URL <https://proceedings.mlr.press/v178/diakonikolas22e.html>.
- [6] Olga Russakovsky, Jia Deng, Hao Su, Jonathan Krause, Sanjeev Satheesh, Sean Ma, Zhiheng Huang, Andrej Karpathy, Aditya Khosla, Michael Bernstein, Alexander C. Berg, and Li Fei-Fei. ImageNet Large Scale Visual Recognition Challenge. *International Journal of Computer Vision (IJCV)*, 115(3):211–252, 2015. doi: 10.1007/s11263-015-0816-y.
- [7] Konstantinos I Tsianos and Michael G Rabbat. Distributed strongly convex optimization. In *2012 50th Annual Allerton Conference on Communication, Control, and Computing (Allerton)*, pages 593–600. IEEE, 2012.
- [8] Tao Yang, Xinlei Yi, Junfeng Wu, Ye Yuan, Di Wu, Ziyang Meng, Yiguang Hong, Hong Wang, Zongli Lin, and Karl H Johansson. A survey of distributed optimization. *Annual Reviews in Control*, 47:278–305, 2019.
- [9] Peva Blanchard, El Mahdi El Mhamdi, Rachid Guerraoui, and Julien Stainer. Machine learning with adversaries: Byzantine tolerant gradient descent. In *Proceedings of the 31st International Conference on Neural Information Processing Systems, NIPS’17*, page 118–128. Curran Associates Inc., 2017. ISBN 9781510860964.
- [10] Sadegh Farhadkhani, Rachid Guerraoui, Nirupam Gupta, Rafael Pinot, and John Stephan. Byzantine machine learning made easy by resilient averaging of momentums. In Kamalika Chaudhuri, Stefanie Jegelka, Le Song, Csaba Szepesvari, Gang Niu, and Sivan Sabato, editors, *Proceedings of the 39th International Conference on Machine Learning*, volume 162 of *Proceedings of Machine Learning Research*, pages 6246–6283. PMLR, 17–23 Jul 2022. URL <https://proceedings.mlr.press/v162/farhadkhani22a.html>.
- [11] Leonardo Bautista-Gomez, Ferad Zyulkyarov, Osman Unsal, and Simon McIntosh-Smith. Unprotected computing: A large-scale study of dram raw error rate on a supercomputer. In *SC’16: Proceedings of the International Conference for High Performance Computing, Networking, Storage and Analysis*, pages 645–655, 2016. doi: 10.1109/SC.2016.54.

- [12] Bianca Schroeder and Garth A. Gibson. Disk failures in the real world: What does an mttf of 1,000,000 hours mean to you? In *Proceedings of the 5th USENIX Conference on File and Storage Technologies*, FAST '07, page 1–es, USA, 2007. USENIX Association.
- [13] Phillipa Gill, Navendu Jain, and Nachiappan Nagappan. Understanding network failures in data centers: Measurement, analysis, and implications. *SIGCOMM Comput. Commun. Rev.*, 41(4):350–361, aug 2011. ISSN 0146-4833. doi: 10.1145/2043164.2018477. URL <https://doi.org/10.1145/2043164.2018477>.
- [14] Gilad Baruch, Moran Baruch, and Yoav Goldberg. A little is enough: Circumventing defenses for distributed learning. In H. Wallach, H. Larochelle, A. Beygelzimer, F. d'Alché-Buc, E. Fox, and R. Garnett, editors, *Advances in Neural Information Processing Systems*, volume 32. Curran Associates, Inc., 2019. URL <https://proceedings.neurips.cc/paper/2019/file/ec1c59141046cd1866bbcbdfb6ae31d4-Paper.pdf>.
- [15] Guosai Wang, Lifei Zhang, and Wei Xu. What can we learn from four years of data center hardware failures? In *2017 47th Annual IEEE/IFIP International Conference on Dependable Systems and Networks (DSN)*, pages 25–36, 2017. doi: 10.1109/DSN.2017.26.
- [16] Devesh Tiwari, Saurabh Gupta, James Rogers, Don Maxwell, Paolo Rech, Sudharshan Vazhkudai, Daniel Oliveira, Dave Londo, Nathan DeBardleben, Philippe Navaux, Luigi Carro, and Arthur Bland. Understanding gpu errors on large-scale hpc systems and the implications for system design and operation. In *2015 IEEE 21st International Symposium on High Performance Computer Architecture (HPCA)*, pages 331–342, 2015. doi: 10.1109/HPCA.2015.7056044.
- [17] Bin Nie, Devesh Tiwari, Saurabh Gupta, Evgenia Smirni, and James H. Rogers. A large-scale study of soft-errors on gpus in the field. In *2016 IEEE International Symposium on High Performance Computer Architecture (HPCA)*, pages 519–530, 2016. doi: 10.1109/HPCA.2016.7446091.
- [18] Sheldon M Ross. *Introduction to probability models*. Academic press, 2014.
- [19] Fanny Yang, Zuowen Wang, and Christina Heinze-Deml. Invariance-inducing regularization using worst-case transformations suffices to boost accuracy and spatial robustness. In H. Wallach, H. Larochelle, A. Beygelzimer, F. d'Alché-Buc, E. Fox, and R. Garnett, editors, *Advances in Neural Information Processing Systems*, volume 32. Curran Associates, Inc., 2019. URL <https://proceedings.neurips.cc/paper/2019/file/1d01bd2e16f57892f0954902899f0692-Paper.pdf>.
- [20] Christina Heinze-Deml and Nicolai Meinshausen. Conditional variance penalties and domain shift robustness, 2017. URL <https://arxiv.org/abs/1710.11469>.
- [21] Saeid Motiian, Marco Piccirilli, Donald A. Adjeroh, and Gianfranco Doretto. Unified deep supervised domain adaptation and generalization. In *IEEE International Conference on Computer Vision (ICCV)*, 2017.
- [22] Sravanti Addepalli, Samyak Jain, et al. Efficient and effective augmentation strategy for adversarial training. *Advances in Neural Information Processing Systems*, 35:1488–1501, 2022.
- [23] Eric Wong, Leslie Rice, and J Zico Kolter. Fast is better than free: Revisiting adversarial training. *arXiv preprint arXiv:2001.03994*, 2020.
- [24] Jeremy Cohen, Elan Rosenfeld, and Zico Kolter. Certified adversarial robustness via randomized smoothing. In *international conference on machine learning*, pages 1310–1320. PMLR, 2019.
- [25] Youssef Allouah, Rachid Guerraoui, Nirupam Gupta, Rafael Pinot, and John Stephan. Distributed learning with curious and adversarial machines. *arXiv preprint arXiv:2302.04787*, 2023.
- [26] Youssef Allouah, Sadegh Farhadkhani, Rachid Guerraoui, Nirupam Gupta, Rafaël Pinot, and John Stephan. Fixing by mixing: A recipe for optimal byzantine ml under heterogeneity. In *International Conference on Artificial Intelligence and Statistics*, pages 1232–1300. PMLR, 2023.

- [27] Sadegh Farhadkhani, Rachid Guerraoui, Nirupam Gupta, Rafael Pinot, and John Stephan. Byzantine machine learning made easy by resilient averaging of momentums. In *International Conference on Machine Learning*, pages 6246–6283. PMLR, 2022.
- [28] P-A Absil. *Optimization algorithms on matrix manifolds*. Princeton University Press, 2008.
- [29] John Wright, Arvind Ganesh, Shankar Rao, Yigang Peng, and Yi Ma. Robust principal component analysis: Exact recovery of corrupted low-rank matrices via convex optimization. *Advances in neural information processing systems*, 22, 2009.
- [30] Matthias Hein and Thomas Bühler. An inverse power method for nonlinear eigenproblems with applications in 1-spectral clustering and sparse pca. *Advances in neural information processing systems*, 23, 2010.
- [31] Rudrasis Chakraborty, Soren Hauberg, and Baba C Vemuri. Intrinsic grassmann averages for online linear and robust subspace learning. In *Proceedings of the IEEE Conference on Computer Vision and Pattern Recognition*, pages 6196–6204, 2017.
- [32] D. Monk. The geometry of flag manifolds. *Proceedings of the London Mathematical Society*, s3-9(2):253–286, 1959. doi: <https://doi.org/10.1112/plms/s3-9.2.253>. URL <https://londmathsoc.onlinelibrary.wiley.com/doi/abs/10.1112/plms/s3-9.2.253>.
- [33] Ke Ye, Ken Sze-Wai Wong, and Lek-Heng Lim. Optimization on flag manifolds. *Mathematical Programming*, 194(1-2):621–660, 2022.
- [34] Nathan Mankovich, Emily J King, Chris Peterson, and Michael Kirby. The flag median and flagirls. In *Proceedings of the IEEE/CVF Conference on Computer Vision and Pattern Recognition*, pages 10339–10347, 2022.
- [35] Kevin P Murphy. *Probabilistic machine learning: an introduction*. MIT press, 2022.
- [36] Massimo Fornasier, Holger Rauhut, and Rachel Ward. Low-rank matrix recovery via iteratively reweighted least squares minimization. *SIAM Journal on Optimization*, 21(4):1614–1640, 2011.
- [37] Toni Karvonen and Chris J Oates. Maximum likelihood estimation in gaussian process regression is ill-posed. *Journal of Machine Learning Research*, 24(120):1–47, 2023.
- [38] Georgios Damaskinos, El-Mahdi El-Mhamdi, Rachid Guerraoui, Arsany Guirguis, and Sébastien Rouault. Aggregator: Byzantine machine learning via robust gradient aggregation. *Proceedings of Machine Learning and Systems*, 1:81–106, 2019.
- [39] Yuxin Chen, Yuejie Chi, Jianqing Fan, Cong Ma, and Yuling Yan. Noisy matrix completion: Understanding statistical guarantees for convex relaxation via nonconvex optimization. *SIAM journal on optimization*, 30(4):3098–3121, 2020.
- [40] Dong Yin, Yudong Chen, Ramchandran Kannan, and Peter Bartlett. Byzantine-robust distributed learning: Towards optimal statistical rates. In *Proceedings of the 35th International Conference on Machine Learning*, volume 80 of *Proceedings of Machine Learning Research*, pages 5650–5659. PMLR, 10–15 Jul 2018.
- [41] Adam Paszke, Sam Gross, Francisco Massa, Adam Lerer, James Bradbury, Gregory Chanan, Trevor Killeen, Zeming Lin, Natalia Gimelshein, Luca Antiga, Alban Desmaison, Andreas Kopf, Edward Yang, Zachary DeVito, Martin Raison, Alykhan Tejani, Sasank Chilamkurthy, Benoit Steiner, Lu Fang, Junjie Bai, and Soumith Chintala. Pytorch: An imperative style, high-performance deep learning library. In *Advances in Neural Information Processing Systems*, volume 32, 2019.
- [42] Rachid Guerraoui, Arsany Guirguis, Jérémy Plassmann, Anton Ragot, and Sébastien Rouault. Garfield: System support for byzantine machine learning (regular paper). In *2021 51st Annual IEEE/IFIP International Conference on Dependable Systems and Networks (DSN)*, pages 39–51, 2021. doi: 10.1109/DSN48987.2021.00021.
- [43] Cong Xie, Oluwasanmi Koyejo, and Indranil Gupta. Generalized byzantine-tolerant sgd, 2018.

- [44] Cong Xie, Oluwasanmi Koyejo, and Indranil Gupta. Phocas: dimensional byzantine-resilient stochastic gradient descent, 2018.
- [45] El Mahdi El Mhamdi, Rachid Guerraoui, and Sébastien Rouault. The hidden vulnerability of distributed learning in Byzantium. In *Proceedings of the 35th International Conference on Machine Learning*, volume 80 of *Proceedings of Machine Learning Research*, pages 3521–3530. PMLR, 10–15 Jul 2018.
- [46] Trishul Chilimbi, Yutaka Suzue, Johnson Apacible, and Karthik Kalyanaraman. Project adam: Building an efficient and scalable deep learning training system. In *Proceedings of the 11th USENIX Conference on Operating Systems Design and Implementation*, OSDI’14, page 571–582, USA, 2014.
- [47] Kaiming He, Xiangyu Zhang, Shaoqing Ren, and Jian Sun. Deep residual learning for image recognition. In *2016 IEEE Conference on Computer Vision and Pattern Recognition (CVPR)*, pages 770–778, 2016. doi: 10.1109/CVPR.2016.90.
- [48] Alex Krizhevsky. Learning multiple layers of features from tiny images, 2009. URL <https://www.cs.toronto.edu/~kriz/learning-features-2009-TR.pdf>.
- [49] Yann LeCun and Corinna Cortes. MNIST handwritten digit database, 2010. URL <http://yann.lecun.com/exdb/mnist/>.
- [50] Ya Le and Xuan S. Yang. Tiny imagenet visual recognition challenge, 2015.
- [51] David Kelly. Rough path recursions and diffusion approximations. *The Annals of Applied Probability*, 26(1):425–461, 2016.
- [52] Jianghong Bao and Qigui Yang. Period of the discrete arnold cat map and general cat map. *Nonlinear Dynamics*, 70(2):1365–1375, 2012.
- [53] Fundamental algorithms for scientific computing in python. <https://scipy.org/>, 2023.
- [54] Nitish Shirish Keskar, Dheevatsa Mudigere, Jorge Nocedal, Mikhail Smelyanskiy, and Ping Tak Peter Tang. On large-batch training for deep learning: Generalization gap and sharp minima. In *International Conference on Learning Representations*, 2017. URL <https://openreview.net/forum?id=H1oyRlYgg>.
- [55] Yang You, Jonathan Hseu, Chris Ying, James Demmel, Kurt Keutzer, and Cho-Jui Hsieh. Large-batch training for lstm and beyond. In *Proceedings of the International Conference for High Performance Computing, Networking, Storage and Analysis*, SC ’19, 2019.
- [56] Kevin Hsieh, Aaron Harlap, Nandita Vijaykumar, Dimitris Konomis, Gregory R. Ganger, Phillip B. Gibbons, and Onur Mutlu. Gaia: Geo-distributed machine learning approaching lan speeds. In *Proceedings of the 14th USENIX Conference on Networked Systems Design and Implementation*, page 629–647, 2017.
- [57] Amedeo Sapio, Marco Canini, Chen-Yu Ho, Jacob Nelson, Panos Kalnis, Changhoon Kim, Arvind Krishnamurthy, Masoud Moshref, Dan Ports, and Peter Richtárik. Scaling distributed machine learning with {In-Network} aggregation. In *18th USENIX Symposium on Networked Systems Design and Implementation (NSDI 21)*, pages 785–808, 2021.
- [58] ChonLam Lao, Yanfang Le, Kshiteej Mahajan, Yixi Chen, Wenfei Wu, Aditya Akella, and Michael Swift. {ATP}: In-network aggregation for multi-tenant learning. In *18th USENIX Symposium on Networked Systems Design and Implementation (NSDI 21)*, pages 741–761, 2021.
- [59] Pat Bosshart, Glen Gibb, Hun-Seok Kim, George Varghese, Nick McKeown, Martin Izzard, Fernando Mujica, and Mark Horowitz. Forwarding metamorphosis: Fast programmable match-action processing in hardware for sdn. In *Proceedings of the ACM SIGCOMM 2013 Conference on SIGCOMM*, SIGCOMM ’13, page 99–110, New York, NY, USA, 2013. Association for Computing Machinery. ISBN 9781450320566. doi: 10.1145/2486001.2486011. URL <https://doi.org/10.1145/2486001.2486011>.

- [60] N McKeown. Pisa: Protocol independent switch architecture. In *P4 Workshop*, 2015.
- [61] Yifan Yuan, Omar Alama, Jiawei Fei, Jacob Nelson, Dan RK Ports, Amedeo Sapio, Marco Canini, and Nam Sung Kim. Unlocking the power of inline {Floating-Point} operations on programmable switches. In *19th USENIX Symposium on Networked Systems Design and Implementation (NSDI 22)*, pages 683–700, 2022.
- [62] Zhouhui Song, Zhenyu Liu, and Dongsheng Wang. Computation error analysis of block floating point arithmetic oriented convolution neural network accelerator design. In *Proceedings of the Thirty-Second AAAI Conference on Artificial Intelligence and Thirtieth Innovative Applications of Artificial Intelligence Conference and Eighth AAAI Symposium on Educational Advances in Artificial Intelligence*, AAAI’18/IAAI’18/EAAI’18. AAAI Press, 2018. ISBN 978-1-57735-800-8.
- [63] Jeremy Bernstein, Jiawei Zhao, Kamyar Azizzadenesheli, and Anima Anandkumar. signsgd with majority vote is communication efficient and fault tolerant. In *7th International Conference on Learning Representations, ICLR 2019, New Orleans, LA, USA, May 6-9, 2019*, 2019.
- [64] Shashank Rajput, Hongyi Wang, Zachary Charles, and Dimitris Papailiopoulos. Detox: A redundancy-based framework for faster and more robust gradient aggregation. In H. Wallach, H. Larochelle, A. Beygelzimer, F. d’Alché-Buc, E. Fox, and R. Garnett, editors, *Advances in Neural Information Processing Systems*, volume 32, 2019.
- [65] Lingjiao Chen, Hongyi Wang, Zachary Charles, and Dimitris Papailiopoulos. DRACO: Byzantine-resilient distributed training via redundant gradients. In *Proceedings of the 35th International Conference on Machine Learning*, volume 80 of *Proceedings of Machine Learning Research*, pages 903–912. PMLR, 10–15 Jul 2018.
- [66] Christian Kümmerle, Claudio Mayrink Verdun, and Dominik Stöger. Iteratively reweighted least squares for basis pursuit with global linear convergence rate. *Advances in Neural Information Processing Systems*, 34:2873–2886, 2021.
- [67] Deeksha Adil, Richard Peng, and Sushant Sachdeva. Fast, provably convergent irls algorithm for p-norm linear regression. *Advances in Neural Information Processing Systems*, 32, 2019.
- [68] Chris M. Bishop. Training with noise is equivalent to tikhonov regularization. *Neural Computation*, 7(1):108–116, 1995. doi: 10.1162/neco.1995.7.1.108.
- [69] Zhun Zhong, Liang Zheng, Guoliang Kang, Shaozi Li, and Yi Yang. Random erasing data augmentation. *Proceedings of the AAAI Conference on Artificial Intelligence*, 34:13001–13008, Apr. 2020. doi: 10.1609/aaai.v34i07.7000. URL <https://ojs.aaai.org/index.php/AAAI/article/view/7000>.
- [70] Terrance DeVries and Graham W Taylor. Improved regularization of convolutional neural networks with cutout. *arXiv preprint arXiv:1708.04552*, 2017.
- [71] Yash Goyal, Tejas Khot, Douglas Summers-Stay, Dhruv Batra, and Devi Parikh. Making the v in vqa matter: Elevating the role of image understanding in visual question answering. *International Journal of Computer Vision*, 127:398–414, 2017.
- [72] Yen-Chun Chen, Linjie Li, Licheng Yu, Ahmed El Kholy, Faisal Ahmed, Zhe Gan, Yu Cheng, and Jingjing Liu. Uniter: Universal image-text representation learning. In *ECCV*, 2020.
- [73] Yu Huang, Chenzhuang Du, Zihui Xue, Xuanyao Chen, Hang Zhao, and Longbo Huang. What makes multimodal learning better than single (provably). In *NeurIPS*, 2021.
- [74] Miguel Sousa Lobo, Lieven Vandenbergh, Stephen Boyd, and Hervé Lebret. Applications of second-order cone programming. *Linear algebra and its applications*, 284(1-3):193–228, 1998.
- [75] Srinadh Bhojanapalli, Nicolas Boumal, Prateek Jain, and Praneeth Netrapalli. Smoothed analysis for low-rank solutions to semidefinite programs in quadratic penalty form. In *Conference on Learning Theory*, pages 3243–3270. PMLR, 2018.

- [76] Chungen Shen, Yunlong Wang, Wenjuan Xue, and Lei-Hong Zhang. An accelerated active-set algorithm for a quadratic semidefinite program with general constraints. *Computational Optimization and Applications*, 78(1):1–42, 2021.
- [77] Ariel Kleiner, Ali Rahimi, and Michael Jordan. Random conic pursuit for semidefinite programming. *Advances in Neural Information Processing Systems*, 23, 2010.
- [78] Hans D Mittelmann. An independent benchmarking of sdp and socp solvers. *Mathematical Programming*, 95(2):407–430, 2003.
- [79] Robert J Vanderbei and Hande Yurttan. Using loqo to solve second-order cone programming problems. *Constraints*, 1(2), 1998.
- [80] Hezhi Luo, Xiaodi Bai, Gino Lim, and Jiming Peng. New global algorithms for quadratic programming with a few negative eigenvalues based on alternative direction method and convex relaxation. *Mathematical Programming Computation*, 11(1):119–171, 2019.
- [81] A Shapiro and JD Botha. Dual algorithm for orthogonal procrustes rotations. *SIAM journal on matrix analysis and applications*, 9(3):378–383, 1988.
- [82] Michel X Goemans and David P Williamson. Improved approximation algorithms for maximum cut and satisfiability problems using semidefinite programming. *Journal of the ACM (JACM)*, 42(6):1115–1145, 1995.
- [83] Steven Diamond and Stephen Boyd. CVXPY: A Python-embedded modeling language for convex optimization. *Journal of Machine Learning Research*, 17(83):1–5, 2016.
- [84] Akshay Agrawal, Robin Verschueren, Steven Diamond, and Stephen Boyd. A rewriting system for convex optimization problems. *Journal of Control and Decision*, 5(1):42–60, 2018.
- [85] Prateek Jain, Purushottam Kar, et al. Non-convex optimization for machine learning. *Foundations and Trends® in Machine Learning*, 10(3-4):142–363, 2017.
- [86] Liqun Qi. Some simple estimates for singular values of a matrix. *Linear algebra and its applications*, 56:105–119, 1984.
- [87] Olga Klopp, Karim Lounici, and Alexandre B. Tsybakov. Robust matrix completion, 2016.
- [88] Cong Xie, Oluwasanmi Koyejo, and Indranil Gupta. Fall of empires: Breaking byzantine-tolerant sgd by inner product manipulation. In Ryan P. Adams and Vibhav Gogate, editors, *Proceedings of The 35th Uncertainty in Artificial Intelligence Conference*, volume 115 of *Proceedings of Machine Learning Research*, pages 261–270. PMLR, 22–25 Jul 2020. URL <https://proceedings.mlr.press/v115/xie20a.html>.
- [89] Zeyuan Allen-Zhu, Faeze Ebrahimianghazani, Jerry Li, and Dan Alistarh. Byzantine-resilient non-convex stochastic gradient descent. In *9th International Conference on Learning Representations, ICLR 2021, Virtual Event, Austria, May 3-7, 2021*. OpenReview.net, 2021. URL <https://openreview.net/forum?id=PbEHqvFtcS>.

A Background and Related Work

Researchers have approached the Byzantine resilience problem from two main directions. In the first class of works, techniques such as geometric median and majority voting try to perform robust aggregation [38], [63], [9]. The other class of works uses redundancy and assigns each worker redundant gradient computation tasks [64], [65].

From another aspect, robustness can be provided on two levels. In weak Byzantine resilience methods such as Coordinate-wise median [40] and Krum [9], the learning is guaranteed to converge. In strong Byzantine resilience, the learning converges to a state as the system would converge in case no Byzantine worker existed. Draco [65] and Bulyan [45] are examples of this class. Convergence analysis of iterated reweighing type algorithms has been done for specific problem classes. For example, [66, 67] show that when IRLS is applied for sparse regression tasks, the iterates can converge linearly. Convergence analysis of matrix factorization problems using IRLS-type schemes has been proposed before, see [36, 39].

It is well known that data augmentation techniques help in improving the generalization capabilities of models by adding more identically distributed samples to the data pool. [19, 20, 21]. The techniques have evolved along with the development of the models, progressing from the basic ones like rotation, translation, cropping, flipping, injecting Gaussian noise [68] etc., to now the sophisticated ones (random erasing/masking [69], cutout [70] etc.). Multi-modal learning setups [71, 72, 73], use different ways to combine data of different modalities (text, images, audio etc.) to train deep learning networks.

B Tractability of Computing Flag Aggregators

In this section, we characterize the computational complexity of solving the Flag Aggregation problem via IRLS type schemes using results from convex optimization. First, we present a tight convex relaxation of the Flag Median problem by considering it as an instantiation of rank constrained optimization problem. We then show that we can represent our convex relaxation as a Second Order Cone Program which can be solved using off-the-shelf solvers [74]. Second, we argue that approximately solving such rank constrained problems in the factored space is an effective strategy using new results from [75] which builds on asymptotic convergence in [36]. Our results highlight that the Flag Median problem can be approximately solved using smooth optimization techniques, thus explaining the practical success of an IRLS type iterative solver.

Interpreting Flag Aggregator (equation 5 in the main paper) in the Case $m = 1$. We first present a convex reformulation of the Flag Aggregator problem (5) in the case when the number of subspaces (or columns) is equal to 1. To make the exposition easier, we will also assume that $\lambda = 0$. With these assumptions, and using the fact that $\|y\|_2 = 1$, each term in the objective function of our FA aggregator in (5) can be rewritten as,

$$\sqrt{(1 - (y^T \tilde{g}_i)^2)} = \sqrt{y^T (I - \tilde{g}_i \tilde{g}_i^T) y} = \|\tilde{B}_i y\|_2, \quad (6)$$

where we use the notation $\tilde{g}_i = g_i / \|g_i\|$ to denote the normalized worker gradients, $I \in \mathbb{R}^{n \times n}$ is the $n \times n$ identity matrix, and \tilde{B}_i is the square root of the matrix $I - \tilde{g}_i \tilde{g}_i^T$. Observe that we can rewrite all the terms in equation (5) in the main paper in a similar fashion as in (6). Furthermore, by relaxing the feasible set to the n -Ball given by $\{y \in \mathbb{R}^n : \|y\|_2 \leq 1\}$, we obtain a Second Order Cone Programming (SOCP) relaxation of our FA problem in (5). SOCP problems can be solved using off-the-shelf packages with open source optimization solvers for gradient aggregation purposes in small scale settings, that is, when the number of parameters $n \approx 10^4$ [76, 77, 78]. Our convex reformulation immediately yields insights on why reweighing type algorithm that was proposed in [34] works well in practice – for example see Section 3 in [79] in which various smoothing functions similar to the Flag Median (square) based smoothing are listed as options. More generally, our SOCP relaxation shows that if the smoothed version can be solved in closed form (or efficiently), then a reweighing based algorithm can be safely considered a viable candidate for aggregation purposes.

Tractable Reformulations when $m > 1$ for Aggregation Purposes. Note that for any feasible Y such that $Y^T Y = I$, we have that the $\text{tr}(Y) = m$.

Remark B.1 (Parametrizing Subspaces using Y .) This assumption is without loss of generality. To see this, first note that in general, a (nondegenerate) subspace \mathcal{S} of a vector space \mathcal{V} is defined as

a subset of \mathcal{V} that is closed under linear combinations. Fortunately, in finite dimensions, we can represent \mathcal{S} as a rectangular matrix M by Fundamental theorem of linear algebra. So, we simply use Y to represent the basis of this matrix M that represents the subspace \mathcal{S} in our FA formulation.

Using this, we can rewrite each term in the objective function of our FA aggregator in equation (5) in the main paper as,

$$\sqrt{\text{tr}\left(Y^T\left(\frac{I}{m}-\frac{g_i g_i^T}{\|g_i\|_2^2}\right)Y\right)}=\sqrt{\text{tr}(Y^T M_i Y)}, \quad (7)$$

where $M_i = M_i^T, i = 1, \dots, p$ is symmetric matrix with *at most one* negative eigenvalue. Optimization problems involving quadratic functions with negative eigenvalues can be solved globally, in some cases [80, 81]. We consider methods that can efficiently (say in polynomial running time in n) provide solutions that are locally optimal. In order to do so, we consider the Semi Definite programming relaxation obtained by introducing matrix $Z \succeq 0 \in \mathbb{R}^{nm \times nm}$ to represent the term YY^T , constrained to be rank one, and such that $\text{tr}(Z) = m$.

By using $\text{vec}(Y) \in \mathbb{R}^{nm}$ to denote the vector obtained by stacking columns of Z , when $m > 1$, we obtain a trace norm constrained SOCP. Importantly, objective function can be written as a sum of terms of the form,

$$\sqrt{\text{vec}(Y)^T(I \otimes M_i)\text{vec}(Y)}=\sqrt{\text{tr}(Z^T(I \otimes M_i))}, \quad (8)$$

where \otimes denotes the usual tensor (or Kronecker) product between matrices.

Properties of lifted formulation in (8). There are some advantages to the loss function as specified in our reformulation (8). First, note that then our relaxation coincides with the usual trace norm based Goemans-Williamson relaxation used for solving Max-Cut problem with approximation guarantees [82]. Albeit, our objective function is not linear, and to our knowledge, it is not trivial to extend the results to nonlinear cases such as ours in (8). Moreover, even when $M_i \succeq 0$, the $\sqrt{\cdot}$ makes the relaxation *nonconvex*, so it is not possible to use off-the-shelf disciplined convex programming software packages such as CVXPY [83, 84]. Our key observation is that away from 0, $\sqrt{\cdot}$ is a *differentiable* function. Hence, the objective function in (8) is differentiable with respect to Z .

Remark B.2 (Using SDP relaxation for Aggregation). In essence, if the optimal solution Z^* to the SDP relaxation is a rank one matrix, then by rank factorization theorem, Z^* can be written as $Z^* = \text{vec}(Y^*)\text{vec}(Y^*)^T$ where $\text{vec}(Y^*) \in \mathbb{R}^{nm \times 1}$. So, after reshaping, we can obtain our optimal subspace estimate $Y^* \in \mathbb{R}^{m \times n}$ for aggregation purposes. In the case the optimal Z^* is not low rank, we simply use the largest rank one component of Z^* , and reshape it to get Y^* .

C Solving Flag Aggregation Efficiently

Convergence Analysis when $m = 1$. Note that for the case $m = 1$, that is, FA provides unit vector $y \in \mathbb{R}^n$ to get aggregated gradient as $yy^T G$, we can use smoothness based convergence results in nonconvex optimization, for example, please see [85]. We believe this addresses most of the standard training pipelines used in practice. Now, we focus on the case with $m > 1$.

Now that we have a smooth reformulation of the aggregation problem that we would like to solve, it is tempting to solve it using first order methods. However, naively applying first order methods can lead to slow convergence, especially since the number of decision variables is now increased to $m^2 n^2$. Standard projection oracles for trace norm require us to compute the full Singular Value Decomposition (SVD) of Z which becomes computationally expensive even for small values of $m, n \approx 10$.

Fortunately, recent results show that the factored form smooth SDPs can be solved in polynomial time using gradient based methods. That is, by setting $Z = \text{vec}(Y)\text{vec}(Y)^T$, and minimizing the loss functions $L_i(Y) = \sqrt{\text{vec}(Y)^T(I \otimes M_i)\text{vec}(Y)}$ with respect to Y , we have that the set of locally optimal points coincide, see [75]. Moreover, we have the following convergence result for first order methods like Gradient Descent that require SVD of $n \times p$ matrices:

Lemma C.1. *If L_i are κ_i -smooth, with a η_i -lipschitz Hessian, then projected gradient descent with constant step size converges to a locally optimal solution to (8) in $\tilde{O}(\kappa/\epsilon^2)$ iterations where $0 \leq \epsilon \leq \kappa^2/\eta$ is a error tolerance parameter, $\kappa = \max_i \kappa_i$, and $\eta = \max_i \eta_i$.*

Above lemma C.1 says that gradient descent will output an aggregation Y that satisfies second order sufficiency conditions with respect to smooth reformulated loss function in (8). All the terms inside \tilde{O} in lemma C.1 are logarithmic in dimensions m, n , lipschitz constant L , and accuracy parameter ϵ . *Remark C.2 (Numerical Considerations).* Note that the lipschitz constant κ of the overall objective function depends on M_i . That is, when M_i has negative eigenvalues, then κ can be high due to the square root function. We can consider three related ways to avoid this issue. First, we can choose a value $m' > m$ in our trace constraint such that $M_i \succeq 0$. Similarly, we can expand (8) (in $\sqrt{\cdot}$) as outer product of columns of Y suggesting that $\tilde{g}\tilde{g}^T$ term need to be normalized by m , thus making $M_i \succeq 0$. Secondly, we can consider adding a quadratic term such as $\|Y\|_{\text{Fr}_0}^2$ to make the function quadratic. This has the effect of decreasing κ and η of the objective function for optimization. Finally, we can use $m_i = \max(k_i, m)$ instead of \min in defining the loss function as in [34] which would also make $M_i \succeq 0$.

D Proof of Lemma C.1 when $m > 1$.

We provide the missing details in Section C when $m > 1$. To that end, we will assume that each worker i provides the server with a list of k_i gradients, that is, $g_i \in \mathbb{R}^{n \times k}$ – a strict generalization of the case considered in the main paper (with $k = 1$), that may be useful independently. Note that in [34], these g_i 's are assumed to be subspaces whereas we do not make that assumption in our FA algorithm.

Now, we will show that the RHS in equation (7) and LHS in equation (8) are equivalent. For that, we need to recall an elementary linear algebra fact relating tensor/Kronecker product, and tr operator. Recall the definition of Kronecker product:

Definition D.1. Let $A \in \mathbb{R}^{d_1 \times d_2}$, $B \in \mathbb{R}^{e_1 \times e_2}$, then $A \otimes B \in \mathbb{R}^{d_1 e_1 \times d_2 e_2}$ is given by,

$$A \otimes B := \begin{bmatrix} a_{1,1}B & \cdots & a_{1,d_2}B \\ \vdots & \ddots & \vdots \\ a_{d_1,1}B & \cdots & a_{d_1,d_2}B \end{bmatrix}, \quad (9)$$

where $a_{i,j}$ denotes the entry at the i -th row, j -th column of A .

Lemma D.2 (Equivalence of Objective Functions). Let $Y \in \mathbb{R}^{n \times m}$, $g \in \mathbb{R}^{n \times k}$ (so, $M \in \mathbb{R}^{n \times n}$). Then, we have that,

$$\text{tr}(Y^T g g^T Y) := \text{tr}(Y^T M Y) = \text{vec}(Y)^T (I \otimes M) \text{vec}(Y), \quad (10)$$

where $I \in \mathbb{R}^{m \times m}$ is the identity matrix.

Proof. Using the definition of tensor product in equation (9), we can simplify the right hand side of equation (10) as,

$$\begin{aligned} \text{vec}(Y)^T (I \otimes M) \text{vec}(Y) &= [y_{11}, \dots, y_{n1}, \dots, y_{1m}, \dots, y_{nm}] \begin{bmatrix} M & 0 & \cdots & 0 \\ \vdots & M & \cdots & \vdots \\ \vdots & \vdots & \ddots & \vdots \\ 0 & \cdots & \cdots & M \end{bmatrix} \begin{bmatrix} y_{11} \\ \vdots \\ y_{n1} \\ \vdots \\ y_{1m} \\ \vdots \\ y_{nm} \end{bmatrix} \\ &= \sum_{j=1}^m y_j^T M y_j \\ &= \sum_{j=1}^m \text{tr}(y_j y_j^T M) = \text{tr}\left(\sum_{j=1}^m y_j y_j^T M\right) = \text{tr}\left(\left(\sum_{j=1}^m y_j y_j^T\right) M\right) \\ &= \text{tr}(Y Y^T M) = \text{tr}(Y^T M Y), \end{aligned} \quad (11)$$

where we used the cyclic property of trace operator $\text{tr}(\cdot)$ in equations (11), and (12) that is, $\text{tr}(ABC) = \text{tr}(CAB) = \text{tr}(BCA)$ for any dimension compatible matrices A, B, C . \square

D.1 Proof of Lemma C.1

Recall that, given $\tilde{M}_i = I \otimes M_i$, the lifted cone programming relaxation of FA can be written as,

$$\min_Z \sum_i \sqrt{\text{tr}(Z^T \tilde{M}_i)} \quad \text{s.t.} \quad Z \succeq 0, \quad \text{tr}(Z) = m, \quad Z = Z^T, \quad (13)$$

where m is the rank of Z or number of columns of Y . We now use the above Lemma D.2 to show that the objective function with respect to Z in the lifted formulation is smooth which gives us the desired convergence result in Lemma C.1.

Proof. let $\tilde{\kappa}_i > 0$,

$$\frac{\partial \sqrt{\text{tr}(Z^T \tilde{M}_i) + \tilde{\kappa}_i}}{\partial Z} = \frac{1}{2\sqrt{\tilde{\kappa}_i + \text{tr}(Z^T \tilde{M}_i)}} \tilde{M}_i, \quad (14)$$

where $\tilde{M}_i = I \otimes M_i$ as in equation (8). Now, since \tilde{M}_i is constant with respect to Z , the gradient term is affected only through a scalar $\sqrt{\text{tr}(Z^T \tilde{M}_i) + \tilde{\kappa}_i}$. So the largest magnitude or entrywise ℓ_∞ -norm of the Hessian is given by,

$$\left| \frac{\partial \frac{1}{\sqrt{\text{tr}(Z^T \tilde{M}_i) + \tilde{\kappa}_i}} \|\tilde{M}_i\|_\infty}{\partial Z} \right| = \frac{\|\tilde{M}_i\|_\infty}{2\sqrt{(\text{tr}(Z^T \tilde{M}_i) + \tilde{\kappa}_i)^3}}. \quad (15)$$

Now, we will argue that the gradient and hessian are lipschitz continuous in the lifted space. Since any feasible $Z \succeq 0$ is positive semidefinite, if $\tilde{M}_i \succeq 0$, then the scalar $\text{tr}(Z^T \tilde{M}_i)$ is at least $m \cdot \lambda_{mn}^{\tilde{M}_i}$ where $\lambda_{mn}^{\tilde{M}_i}$ is the smallest (or mn -th) eigenvalue of \tilde{M}_i . So, we can choose $\tilde{\kappa}_i = 0 \forall i$. If not, then there is a negative eigenvalue, possibly repeated. So, the gradient might not exist. In cases where \tilde{M}_i has negative eigenvalues, we can choose $\tilde{\kappa}_i = \tilde{\kappa} = \left| \min_i \min(\lambda_{mn}^{\tilde{M}_i}, 0) \right|$. With these choices, we have that the gradient of the objective function in (8) is lipschitz continuous. By a similar analysis using the third derivative, we can show that Hessian is also lipschitz continuous with respect to Z . In other words, all the lipschitz constant of both the gradient and hessian of our overall objective function is controlled by $\tilde{\kappa} > 0$. Hence, we have all conditions satisfied required for Lemma 1 in [75], and we have our convergence result for FA in the factored space of $\text{vec}(Y)$. \square

Few remarks are in order with respect to our convergence result. First, **is the choice $\tilde{\kappa}$ important for convergence?** Our convergence result shows that a perturbed objective function $\text{tr}(Z^T \tilde{M}_i) + \tilde{\kappa}$ has the same second order stationary points as that of the objective function in the factored form formulated using Y (or $\text{vec}(Y)$). We can avoid this perturbation argument if we explicitly add constraints $\text{tr}(Z^T \tilde{M}_i) \geq 0$, since projections on linear constraints can be performed efficiently exactly (sometimes) or approximately. Note that these constraints are natural since it is not possible to evaluate the square root of a negative number. Alternatively, we can use a smooth approximate approximation of the absolute values $\sqrt{|\text{tr}(Z^T \tilde{M}_i)|}$. In this case, it is easy to see from (14), and (15) that the constants governing the lipschitz continuity as dependent on the absolute values of the minimum eigenvalues, as expected. In essence, no, the choice of $\tilde{\kappa}$ does not affect the nature of landscape – approximate locally optimal points remain approximately locally optimal. In practice, we expect the choice of $\tilde{\kappa}$ to affect the performance of first order methods.

Second, **can we assume $\tilde{M}_i \succ 0$ for gradient aggregation purposes?** Yes, this is because, when using first order methods to obtain locally optimal solution, the scale or norm of the gradient becomes a secondary factor in terms of convergence. So, we can safely normalize each M_i by the nuclear norm $\|M_i\|_* := \sum_{j=1}^{k_i} \sigma_j$ where σ_j is the j -th singular value of M_i . This ensures that $I - M_i \succeq 0$, assistant convergence. While $\|M_i\|_*$ itself might be computationally expensive to compute, we may be able to use estimates of $\|M_i\|_*$ via simple procedures as in [86]. In most practical implementations including ours, we simply compute the average of the gradients computed by each worker before

sending it to the parameter server, that is, $k_i \equiv k = 1$ in which case simply normalizing by the euclidean norm is sufficient for our convergence result to hold. Our FA based distributed training Algorithm 1 solves the factored form for gradient aggregation purposes (in Step 6) at the parameter server.

Finally, please note that our technical assumptions are standard in optimization literature, that exploits smoothness of the objective function – since the feasible set of Y in (1) is bounded, assumptions are satisfied. Our proof techniques are standard, and we simply use them on our reformulation to obtain convergence guarantee *second order stationary points* for IRLS iterations since there exists a tractable SDP relaxation.

D.2 FA Optimality Conditions and Similarities with Bulyan [45] Baseline.

We first restate our Flag Aggregator with $g_i \in \mathbb{R}^{n \times k}$ in optimization terms as follows,

$$\min_{Y: Y^T Y = I} A(Y) := \sum_{i=1}^p \sqrt{\left(1 - \frac{\text{tr}(Y^T g_i g_i^T Y)}{\text{tr}(g_i^T g_i)}\right)} + \lambda \mathcal{R}(Y), \quad (16)$$

and write its associated Lagrangian \mathcal{L} defined by,

$$\mathcal{L}(Y, \Gamma) := \sum_{i=1}^p \sqrt{\left(1 - \frac{\text{tr}(Y^T g_i g_i^T Y)}{\text{tr}(g_i^T g_i)}\right)} + \lambda \mathcal{R}(Y) + \text{tr}(\Gamma^T (Y^T Y - I)), \quad (17)$$

where $\Gamma \in \mathbb{R}^{m \times m}$ denotes the Lagrange multipliers associated with the orthogonality constraints in equation (16). In particular, since the constraints we have are equality, there are no sign restrictions on Γ , so they are often referred to as “free”. Moreover, since Y is a real matrix, the constraints are symmetric (i.e., $y_i^T y_j = y_j^T y_i$), we may assume that $\Gamma = \Gamma^T$, without loss of generality.

We will introduce some notations to make calculations easier. We will use $\tilde{g}_i \in \mathbb{R}^{n \times k}$ to denote the normalized gradients matrix of the data terms in equation (16). That is, we define

$$\tilde{g}_i := \frac{1}{\text{tr}(g_i^T g_i) \cdot \sqrt{\left(1 - \frac{\text{tr}(Y^T g_i g_i^T Y)}{\text{tr}(g_i^T g_i)}\right)}} g_i g_i^T =: d_i g_i g_i^T. \quad (18)$$

With this notation, we are ready to use the first optimality conditions associated with the constrained optimization problem in (16) with its Lagrangian in (17) By first order optimality or KKT conditions, we have that,

$$\begin{aligned} 0 &= \nabla_Y \mathcal{L}(Y_*, \Gamma_*) = \left(\sum_{i=1}^p \tilde{g}_i \tilde{g}_i^T \right) Y_* + \lambda \nabla \mathcal{R}(Y_*) + 2Y_* \Gamma_* \\ &= G D_* G^T Y_* + \lambda \nabla \mathcal{R}(Y_*) + 2Y_* \Gamma_*, \quad (\text{Objective}) \\ 0 &= \nabla_{\Gamma} \mathcal{L}(Y_*, \Gamma_*) = Y_*^T Y_* - I, \quad (\text{Feasibility}) \end{aligned} \quad (19)$$

where $Y_* \in \mathbb{R}^{n \times m}$, $\Gamma_* \in \mathbb{R}^{m \times m}$ are the optimal primal parameters, lagrangian multipliers, and $D_* \in \mathbb{R}_{>0}^{p \times p}$ is the diagonal matrix with entries equal to $-d_i < 0$ as in equation (18). We may ignore the Feasibility conditions since our algorithm returns an orthogonal matrix by design, and focus on the Objective conditions. Now, by bringing the term associated with Lagrangian to the other side, and then right multiplying by Γ_*^{-1} inverse of Γ_* , we have that Y_* satisfies the following identity,

$$Y_* = -\frac{1}{2} (G D_* G^T Y_* + \lambda \nabla \mathcal{R}(Y_*)) \Gamma_*^{-1}. \quad (20)$$

By using the identity (20), we can write an equivalent representation of our aggregation rule $Y_* Y_*^T G$ given by,

$$\begin{aligned}
Y_* Y_*^T G &= \frac{1}{4} \underbrace{(GD_* G^T Y_* + \lambda \nabla \mathcal{R}(Y_*)) \Gamma_*^{-1} \Gamma_*^{-1} (Y_*^T G D_* G^T + \lambda \nabla \mathcal{R}(Y_*)^T)}_{:= \mathfrak{M}_* \in \mathbb{R}^{m \times p}} G \\
&\propto (GD_* G^T Y_* + \lambda \nabla \mathcal{R}(Y_*)) \mathfrak{M}_* \\
&= G \underbrace{D_* G^T Y_*}_{:= S'_* \in \mathbb{R}^{p \times m}} \mathfrak{M}_* + \lambda \nabla \mathcal{R}(Y_*) \mathfrak{M}_* \\
&= G S'_* \mathfrak{M}_* + \lambda \nabla \mathcal{R}(Y_*) \mathfrak{M}_* \\
&:= G S_{\text{FA}} + \lambda \nabla \mathcal{R}(Y_*) \mathfrak{M}_*, \tag{21}
\end{aligned}$$

that is, the update rule of FA can be seen as a left multiplication with the square “flag selection” matrix $S_{\text{SA}} = S'_* \mathfrak{M}_* \in \mathbb{R}^{p \times p}$, and then perturbing with the gradient $\nabla \mathcal{R}(Y_*)$ of the regularization function \mathcal{R} with a different matrix \mathfrak{M}_* as in equation (21). Importantly, we can see in equation (21) that the (reduced) selection matrix $S \in \mathbb{R}_{\geq 0}^{p \times m}$ in Bulyan [45] is equivalent to the total selection matrix $S_{\text{SA}} \in \mathbb{R}^{p \times p}$ in our FA setup. Moreover, we can also see that domain knowledge in terms of regularization function may also determine the optimal subspace, albeit additively only. We leave the algorithmic implications of our result as future work.

Remark D.3 (Invertibility of Γ_* in Equation (20).). Theoretically, note that Γ is symmetric, so by Spectral Theorem, we know that its eigen decomposition exists. So, we may use pseudo-inverse instead of its inverse. Computationally, given any primal solution Y_* we can obtain Γ_* by left multiplying equation (19) by Y_* and use feasibility i.e., $Y_*^T Y_* = I$. Now, we obtain Γ_*^{-1} columnwise by using some numerical solver such as conjugate gradient (with fixed iterations) on Γ with standard basis vectors. In either case, our proof can be used with the preferred approximation choice of Γ_*^{-1} to get the equivalence as in equation (21).

Remark D.4 (Provable Robustness Guarantees for FA.). Since our FA scheme is based on convexity, it is possible to show worst-case robustness guarantees for FA iterations under mild technical conditions on Y^* – even under correlated noise, see for e.g. Assumption 1 in [87]). In fact, by using the selection matrix S_{FA} in equation (21) in Lemma 1 in [38] and following the proof, we can get similar provable robustness guarantees for FA. We leave the theoretical analysis as future work.

E ADDITIONAL EXPERIMENTS

E.1 The Effect of Regularization Parameter

Our algorithm depends on the regularization parameter λ . Figure 11 below illustrates the effect of this parameter on similarity of aggregated gradient vectors for FA and Multi-Krum. For this experiment, we sample the gradients output by the parameter server across multiple epochs for both FA and Multi-Krum and compute the cosine similarity of corresponding vectors. We repeat the experiment with different λ values. As we can see, for smaller iterations there is some similarity between the gradients computed by FA and Multi-Krum. This similarity is more visible for smaller λ values.

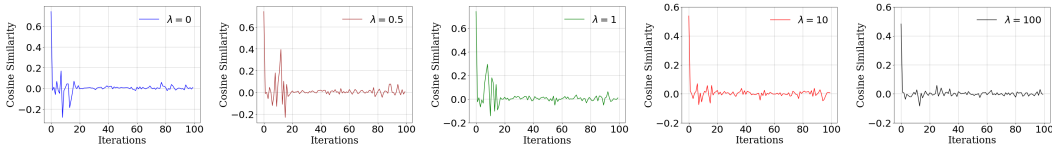


Figure 11: The effect of the regularization parameter λ on similarity of FA performance to Multi-Krum

E.2 Experiments with other Byzantine attacks or baselines

So far we have presented results where Byzantine workers send uniformly random gradient vectors, use synthetic data (nonlinear data augmentation routines), or where a percentage of gradients are

dropped and zeroed out at the parameter server to show tolerance to communication loss. Here we provide more results when Byzantine workers send a gradient based on the Fall of Empires attack with $\epsilon = 0.1$ [88] in Figure 12a and when they send 10x amplified sign-flipped gradients [89] in Figure 12b. Because mathematically, one iteration of FA with uniform weights assigned across all workers is equivalent to PCA, we also add a baseline for top- m principal components of the gradient matrix in Figure 12c. The novelty in our FA approach is the extension of PCA to an iteratively reweighted form that is guaranteed to converge. Specifically, we show that we obtain a convergent procedure in which we repeatedly solve weighted PCA problems. Moreover, the convergence guarantee immediately follows when the procedure is viewed as an IRLS procedure solving the MLE problem induced by the value of workers modeled with a beta distribution as in Section 2.2.

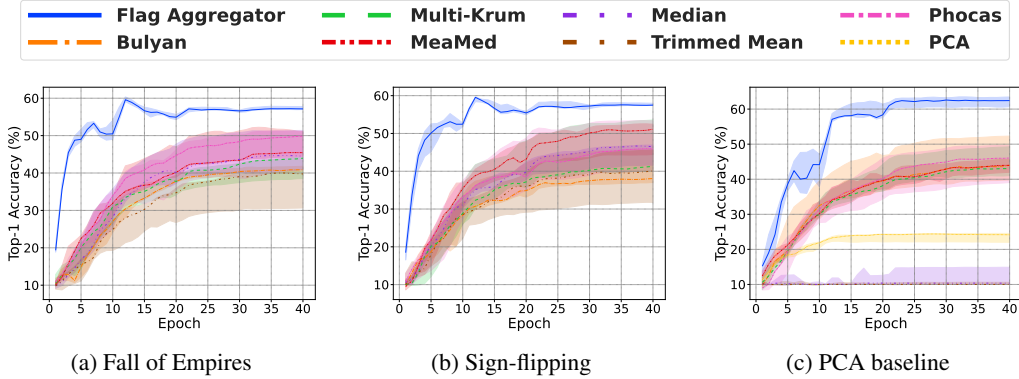


Figure 12: Robustness towards other Byzantine attacks, $p = 15$, $f = 2$.

E.3 Experiments with the Tiny ImageNet dataset

We repeated our experiments with Tiny ImageNet [50] which contains 100000 images of 200 classes (500 for each class) downsized to 64×64 colored images. We fix our batch size to 192 and use ResNet-50 [47] throughout the experiments.

Tolerance to the number of Byzantine workers: In this experiment, we have $p = 15$ workers of which $f = 1, \dots, 3$ are Byzantine and send random gradients. The accuracy of test data for FA in comparison to other aggregators is shown in Figure 13. As we can see, for $f = 1$ and $f = 2$, FA converges at a higher accuracy than all other schemes. For all cases, FA also converges in $\sim 2x$ less number of iterations.

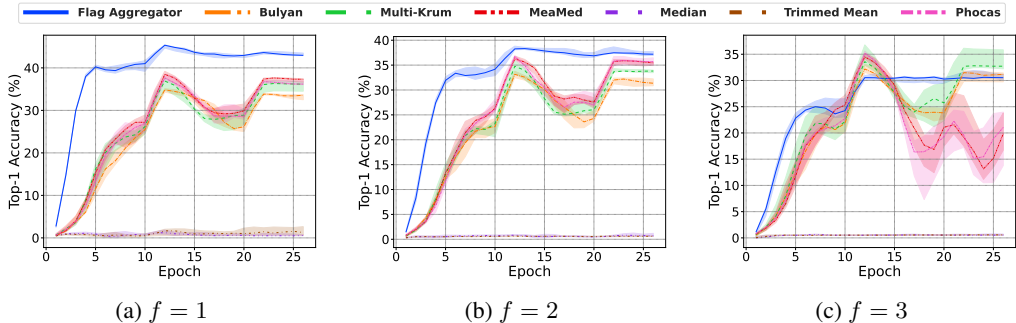


Figure 13: Tolerance to the number of Byzantine workers for robust aggregators.

Tolerance to communication loss: We set a 10% loss rate for the links connecting $f = 1, \dots, 3$ of the workers to the parameter server. Figure 14 shows that our takeaways in the main paper are also confirmed in this setting with the new dataset.

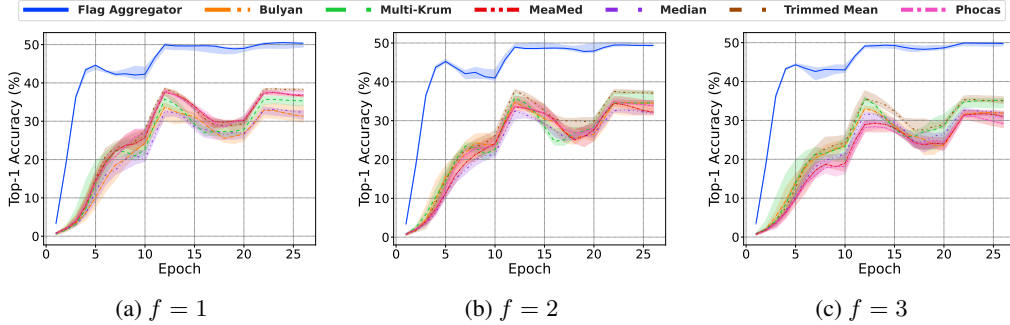


Figure 14: Tolerance to communication loss

The effect of having augmented data during training in Byzantine workers: We choose two non linear augmentation schemes, Lotka Volterra (shown in rows 1 and 3 of Figure 15) and Arnold’s Cat Map (shown in rows 2 and 4 of Figure 15).

As seen from the figure, Arnold’s Cat Map augmentations stretch the images and rearrange them within a unit square, thus resulting in streaky patterns. Whereas the Lotka Volterra augmentations distort the images while keeping the images similar to the original ones. We perform experiments with data augmented with varying shares using the two methods and show the results in Figure 16. For CIFAR-10, we showed the results when all of the samples in Byzantine workers are augmented in Figure 7 in the main paper. For Tiny ImageNet, this case is shown Figure 16a. Figures 16b and 16c show the results under different ratios on CIFAR-10. By changing the ratios we were interested to see if streaky patterns augmented by Arnold’s Cat Map would introduce a more adverse effect from Byzantine workers compared to Lotka Volterra. Although the results do not show a significant signal, we can see that the augmentations did impact the overall gradients and that FA performs significantly better.



Figure 15: TinyImagenet data with Augmentation: **Row 1:** Lotka Volterra augmentation on Class Horse. **Row 2:** Arnold’s Cat Map augmentation on Class Horse. **Row 3:** Lotka Volterra augmentation on Class Ship. **Row 4:** Arnold’s Cat Map augmentation on Class Ship.

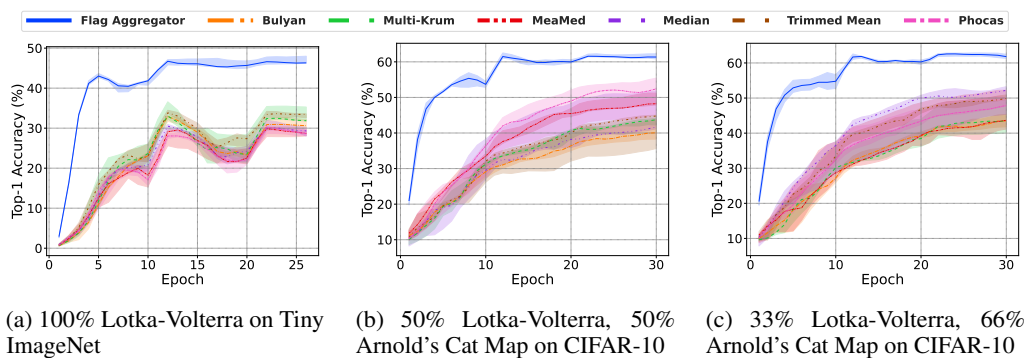


Figure 16: Accuracy of using augmented data in $f = 3$ workers